Bidirectional Reflectance of H_2O Cryofilms on Specular and Diffusing Surfaces

A. M. Smith* and B. E. Wood†
ARO, Inc., Arnold Air Force Station, Tenn.
and
L. S. Fletcher‡
University of Virginia, Charlottesville, Va.

The bidirectional reflectance of monochromatic visible and near-infrared radiation from H_2O cryofilms on polished copper and black epoxy paint surfaces is measured in the plane of incidence for several film thicknesses, zenith incidence angles, and wavelengths. It is observed that the reflectance distributions retain a significant specular peak even for an H_2O film thickness of 500 μ. For large incidence angles, superspecular maxima occur in the bidirectional reflectance distributions for H_2O cryofilms on black paint substrates but not for H_2O films on polished copper. The angular displacement of the superspecular peaks from the specular direction depends upon the film thickness in a nonmonotonic manner.

Introduction

THE manner in which H_2O cryofilms affect the visible and near-infrared (IR) reflection properties of cryogenically cooled surfaces is of interest for several reasons. Probably the most timely one is that these cryofilms can form on the cold mirror surfaces of optical systems operating in a cryogenic environment and may alter significantly the bidirectional reflectance of the mirrors, as well as their specular reflectance. This would, of course, have an appreciable effect on the performance of the optical system. A second reason is that the presence of H_2O films on the black-painted cryopanels of a space simulation chamber may modify appreciably the bidirectional reflectance of these surfaces and also change their directional-hemispherical reflectance. Thus, the directional characteristics and magnitude of the solar simulator irradiance reflected from the cryopanels might be altered significantly and hence adversely influence the results of a space simulation experiment. Previously, the monochromatic absolute hemispherical-directional reflectance (equal to directional-hemispherical reflectance through reciprocity) was measured for H_2O and CO_2 cryodeposits on polished stainless steel and black paint cryosurfaces.[1,2] In addition, the angular distribution of total visible and near-IR radiation reflected from CO_2 films on polished copper and black epoxy paint substrates has been measured,[3] as well as the monochromatic bidirectional reflectance.[4] The objective of this paper is to present the bidirectional reflectance of monochromatic visible and near-IR radiation in the plane of incidence from H_2O cryofilms formed on polished copper and black paint surfaces.

Bidirectional Reflectance

The bidirectional reflection of radiation from a cryofilm was measured by the method shown in Fig. 1. In this technique, the film is illuminated with a collimated beam of radiant flux $e_i(\psi)$ at a zenith incidence angle ψ. Reflected radiant flux leaving the film of thickness τ through a solid angle $\Delta\omega_r$ in the direction defined by the zenith reflection angle θ and the plane of incidence is designated as $E(\psi,\theta,\tau)$ and is measured by the detector. Note that the zenith incidence angle and zenith reflection angle are measured from the surface normal. One can define the bidirectional reflectance of the film-substrate surface system as $\rho_{bd}(\psi,\theta,\tau) = I_r(\psi,\theta,\tau)/e_i/\pi$, where $(I_r\psi,\theta,\tau)$ is the reflected radiant intensity, which is related to the reflected flux by

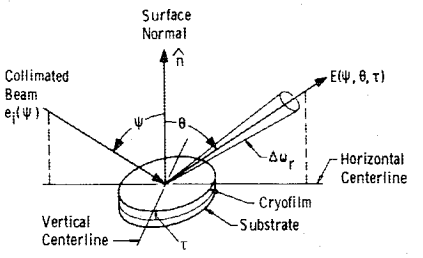

Fig. 1 Bidirectional technique.

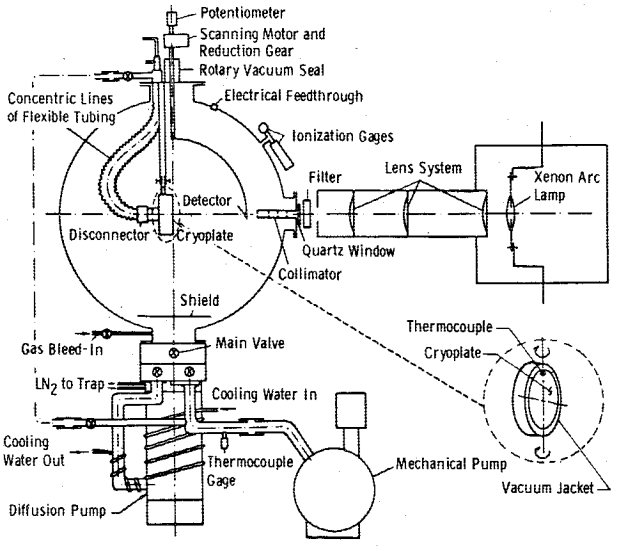

Fig. 2 Experimental apparatus.

Received Nov. 11, 1977; presented as Paper 78-88 at the AIAA 16th Aerospace Sciences Meeting, Huntsville, Ala., Jan. 16-18, 1978.

Index categories: Radiation and Radiative Heat Transfer; Thermal Surface Properties; Thermophysical Properties of Matter.

*Research Supervisor, von Kármán Gas Dynamics Facility. Associate Fellow AIAA.

†Research Engineer, von Kármán Gas Dynamics Facility. Associate Fellow AIAA.

‡Professor and Chairman, Department of Mechanical Engineering. Associate Fellow AIAA.

$E = I_r \cos\theta \Delta\omega_r$. Physically, this bidirectional reflectance definition can be interpreted as the ratio of the intensity reflected by an actual surface system at angle θ in the plane of incidence to the intensity that would be reflected in the same direction by a surface system that was perfectly reflecting and uniformly diffusing.

Experimental Apparatus

All bidirectional reflectance experiments were conducted in a spherical vacuum chamber that contained a liquid-nitrogen (LN_2)-cooled cryoplate, as shown in Fig. 2. To minimize internal reflections, all interior surfaces of the chamber except the cryoplate were painted flat black. The pumping system for the chamber consisted of a mechanical forepump and a 6-in. oil diffusion pump equipped with an LN_2 cold trap. Pressures of 10^{-7} Torr could be obtained with this system. Chamber pressures were measured with a thermal ionization gage at pressures below 10^{-3} Torr and with an alpha particle ionization gage at pressures above 10^{-3} Torr. The copper cryoplate located in the center of the chamber and the LN_2 lines leading to it were shielded completely by a vacuum jacket except for the flat front face of the cryoplate, where the cryofilms were formed. This face was polished to an rms surface roughness σ of approximately 0.01 μ. It was used as the test surface and either was coated with black epoxy paint or was just the bare polished copper. A copper-constantan thermocouple was attached to the test surface to measure the deposition temperature. The test surface could be rotated about its vertical centerline to obtain any desired polar angle between the collimated beam of incident radiation and the test surface normal. As shown in the schematic, the collimated irradiance was obtained from a xenon arc lamp by means of a system of lenses and apertures. Monochromatic irradiance could be obtained by inserting narrow-bandpass interference filters into the radiation beam. These filters typically had a bandwidth at half-maximum transmission of 0.015 μ ($\pm$0.007 μ). All bidirectional reflectance measurements were made using a silicon solar cell detector mounted on a remotely rotatable arm (see Fig. 2). Water vapor was introduced into the chamber at a constant rate by allowing degassed distilled water to evaporate under vacuum from a reservoir and then pass through a rotameter and needle valve.

Experimental Procedure

After the vacuum chamber had been evacuated to a pressure of about 1×10^{-7} Torr and the xenon lamp turned on, a transmission filter of a certain wavelength λ was inserted into the radiation beam and the test surface rotated to the desired zenith incidence angle ψ. Then, with the test surface still at 300 K, the detector was rotated about it in the plane of incidence, and a reference trace of the bidirectional distribution of the reflected radiant flux was made for the surface when no cryofilm was present ($\tau = 0$). The test surface was rotated to other values of ψ and the mapping procedure repeated for various wavelengths. Next, the cryoplate was cooled to 77 K, and, after valving off the chamber from the pumping system, a cryofilm was formed continuously on the test surface by flowing H_2O vapor into the chamber at a constant rate. The deposition rate $\dot{\tau}$ for the cryofilm was measured in situ by recording thin-film interference patterns for two different incidence angles.[3,5,6] With the constant deposition rate known, a cryofilm layer of specified thickness τ was formed by flowing vapor into the chamber for a specified time. The thickness of this layer always was chosen larger than the maximum film thickness at which thin-film interference was observed. Throughout deposition, the chamber pressure p was approximately 4×10^{-4} Torr. After the vapor flow was stopped, bidirectional distributions of the reflected radiant flux were recorded for various incidence angles and wavelengths. Then, the vapor again was added to the chamber, forming another cryofilm layer on top of the first, and bidirectional distribution measurements were made again. This procedure was repeated and bidirectional distribution measurements made for each resulting film thickness.

Bidirectional Reflectance for H_2O Films on Polished Copper

Figure 3 presents the relative bidirectional reflectance for various thicknesses of H_2O films formed on a polished copper substrate. These results are for a zenith incidence angle of 11 deg and irradiance wavelengths of $\lambda = 0.7$, 0.9, and 1.1 μ. The reflectance values of less than 0.012 in Fig. 3 are displayed on a greatly increased scale in Fig. 4. As shown in Figs. 3 and 4, the presence of H_2O cryofilms on a polished copper substrate causes the reflectance in the specular direction ($\theta = 11$ deg) to decrease drastically for film thicknesses of 20 μ and larger, with the greatest decrease occurring at the shortest wavelength. For the 20μ-thick film, the specular peak value for $\lambda = 0.7$ μ decreased from 1.0 to approximately 0.37, whereas for $\lambda = 0.9$ μ, the same film thickness reduced the specular peak from 1.0 to approximately 0.53. For the 60-μ-thick film, the specular value was reduced considerably more to 0.04 for $\lambda = 0.7$ μ, as compared to 0.13 for $\lambda = 0.9$ μ. These comparisons indicate that more of the short-wavelength radiation is scattered out of the direct beam than is the longer-wavelength radiation. This large decrease in the specular peak with increasing film thickness and/or decreasing wavelength results from increased scattering, which also causes an accompanying increase in the bidirectional reflectance in nonspecular directions. As the film thickens, the reflectance distributions become increasingly nonspecular but do not become diffuse for the thicknesses investigated. Such behavior can be explained by noting that both surface and internal scattering by the cryofilms cause the incident monochromatic radiation to be reflected in directions other than just the specular direction. At first, when the film is relatively thin, the surface scattering likely will predominate. However, as the film thickens, the internal scattering becomes increasingly significant, thereby causing the reflectance distribution to become even more diffuse. However, the presence of a well-defined specular peak still can be observed even for the 100-μ-thick film at $\lambda = 0.7$ μ in Fig. 4. Also ob-

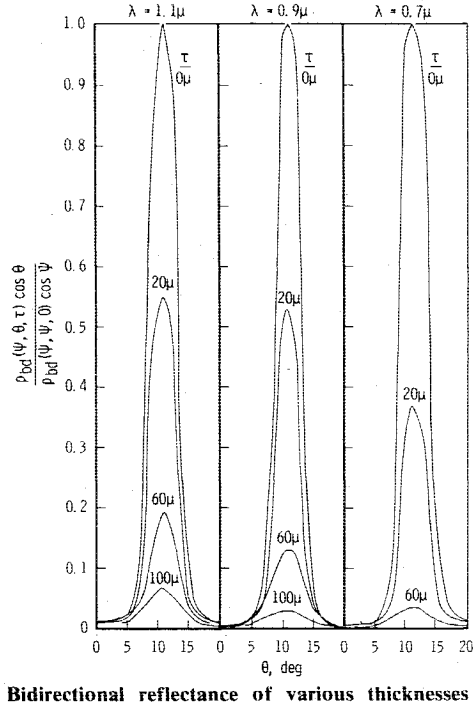

Fig. 3 Bidirectional reflectance of various thicknesses of H_2O cryofilms on a polished copper substrate for various radiation wavelengths and an incidence angle of 11 deg.

served in Fig. 4 for a 20-μ-thick film are the scattering interference peaks[3] that occur in the bidirectional reflectance distributions for relatively thin cryofilms formed on a specularly reflecting substrate. These peaks (and valleys) are a result of interference that is generated by scattering of the incident radiation at the vacuum-cryofilm interface. This phenomenon has been investigated and analyzed in detail in Ref. 3.

The bidirectional reflection distributions obtained for H_2O cryofilms on polished copper using a large irradiance incidence angle of $\psi = 55$ deg are shown in Fig. 5. These results are for monochromatic irradiance of 0.7-, 0.9-, and 1.1-μ wavelengths and are presented in a manner similar to that of Fig. 4. For this large incidence angle, it is observed that the specular peak decreases, and the reflection distributions become more diffuse with increasing film thickness in a manner similar to that observed for $\psi = 11$ deg. There are, however, some phenomena observed in the distributions for the large incidence angle that were not readily apparent in the distributions for the small incidence angle. One of the these is the "backscattering" of reflected radiation into the quadrant of incidence ($\theta < 0$ deg) in the general direction of the irradiance, $\theta \simeq -\psi$. As shown in Fig. 5, this phenomenon is observed primarily for relatively thin films. Another interesting difference between the distributions for large and small incidence angles is noted when comparing the results of Figs. 3 and 5 for $\lambda = 0.7$ μ. For the 20-μ-thick film and $\psi = 11$ deg, the specular peak in Fig. 3 reaches a peak height of 0.37, whereas for the same 20-μ-thick film and for $\psi = 55$ deg, the peak height is only about 0.11 (off scale in Fig. 5). This can be explained by the specular peak for these incidence angles being due primarily to the reflection of the radiation from the copper substrate. The higher incidence angle ($\psi = 55$ deg) results in a greater path length for the radiation to pass through inside the film, thereby causing a greater amount of extinction by internal scattering and hence reducing the amount of energy emerging from the film in the specular direction. For $\lambda = 0.9$ μ and $\tau = 20$ μ, the specular peak height of 0.45 for $\psi = 55$ deg (off scale in Fig. 5) is only slightly less than the value of 0.53 for $\psi = 11$ deg in Fig. 3, since the 0.9-μ radiation is not scattered nearly so much as the 0.7-μ radiation. Another aspect to the incidence angle effects is the scattering interference patterns observed in Fig. 4 for $\psi = 11$ deg and a film thickness of 20 μ. As shown in Fig. 5, no such patterns were observed for the same film thickness for an incidence angle of 55 deg. The decrease in surface scattering with increasing incidence angle is the primary reason why no interference patterns were observed for $\psi = 55$ deg. As pointed out in Ref. 3, scattering from the vacuum-film interface is required for genereting this type of interference pattern.

Figure 6 presents the effect of irradiance wavelength on the bidirectional reflectance of a 1000-μ-thick water cryofilm on

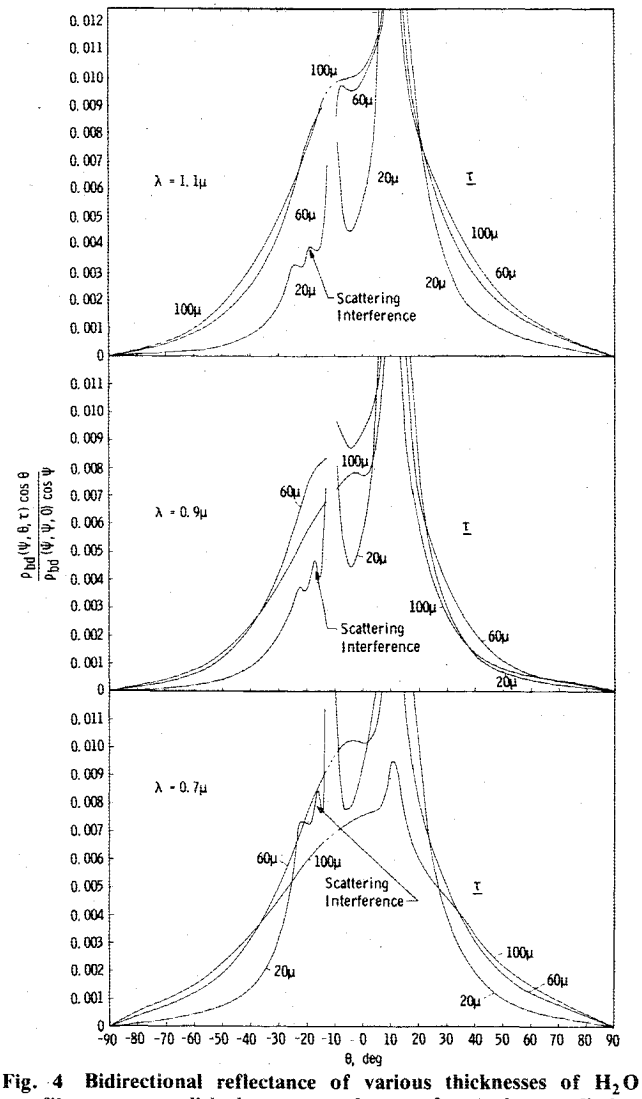

Fig. 4 Bidirectional reflectance of various thicknesses of H_2O cryofilms on a polished copper substrate for various radiation wavelengths and an incidence angle of 11 deg. (Note greatly expanded ordinate scale label.)

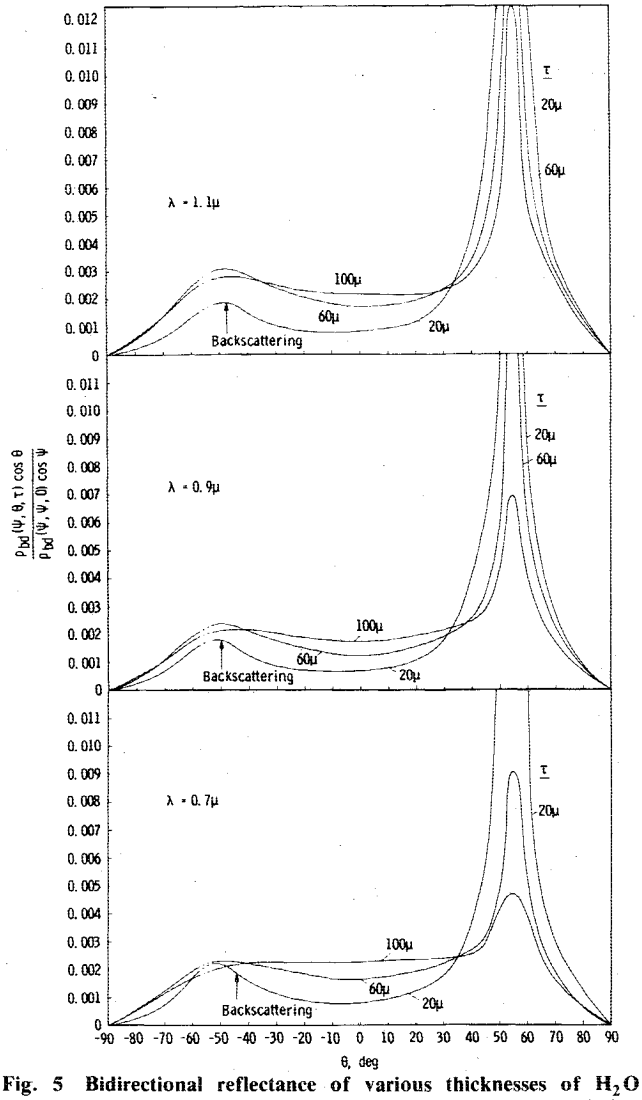

Fig. 5 Bidirectional reflectance of various thicknesses of H_2O cryofilms on a polished copper substrate for various radiation wavelengths and an incidence angle of 55 deg. (Note greatly expanded ordinate scale label.)

polished copper for incidence angles of 22 and 66 deg. It is observed that even for a 1000-μ-thick H_2O film the specular peak is still present for all wavelengths shown. It is noted in Fig. 6 that the bidirectional reflectance for the 0.6-μ wavelength is greater than that for the other wavelengths. By carefully comparing the bidirectional reflectances for the other wavelengths from 0.7 to 1.1 μ, it is found that they decrease with wavelength until reaching a minimum for the 0.9-μ radiation. An increase in bidirectional reflectance is then seen for the 1.0- and 1.1-μ wavelengths, which indicates that an absorption band occurs in the neighborhood of the 0.9-μ wavelength. This band has been observed previously for some other water cryodeposits.[6]

Bidirectional Reflectance for H_2O Films on Black Paint

Figures 7 and 8 present the bidirectional reflectance of total visible and near-IR radiation from H_2O films formed on a black expoxy paint substrate. The results shown are for incidence angles of 0, 33, 55, and 66 deg and film thicknesses ranging from 10 to 500 μ. For increasing H_2O film thicknesses up to 50 μ, the bidirectional reflectance in the specular direction is reduced greatly. However, even for a film thickness of 50 μ, the peak in the specular direction is still relatively well defined. Just as for the H_2O film formed on polished copper, this decrease of the peak in the reflection distribution and the accompanying increase in the bidirectional reflectance in nonspecular directions is due to surface and internal scattering. As the film thickens, the internal scattering becomes increasingly significant. This effect is illustrated vividly in Figs. 7 and 8 by noting that an increase in film thickness from 50 to 500 μ causes the bidirectional reflectance in most all directions ($\theta \neq \pm 90$ deg) to increase greatly. For an H_2O film on black paint, the reflection distributions do not become completely diffuse for any thickness investigated, since a peak always is observed in the reflection distributions, as shown in Figs. 7 and 8. It also is observed in Figs. 7 and 8 that the peaks in the bidirectional reflectance distributions first decrease and then increase as the films thicken and the reflection distributions become more diffuse. Note that the reflection distributions shown in Fig. 8 for the large incidence angles, 55 and 66 deg, are not as diffuse as those shown in Fig. 7 for the smaller incidence angles, 0 and 33 deg. Also, notice in Fig. 8, for $\psi = 55$ and 66 deg, that the peaks or maxima in the bidirectional reflectance distributions for the film thicknesses up to 50 μ occur at zenith reflection angles that are greater than the specular reflection angles. Following Ref. 7, these types of peaks will be referred to as superspecular maxima.

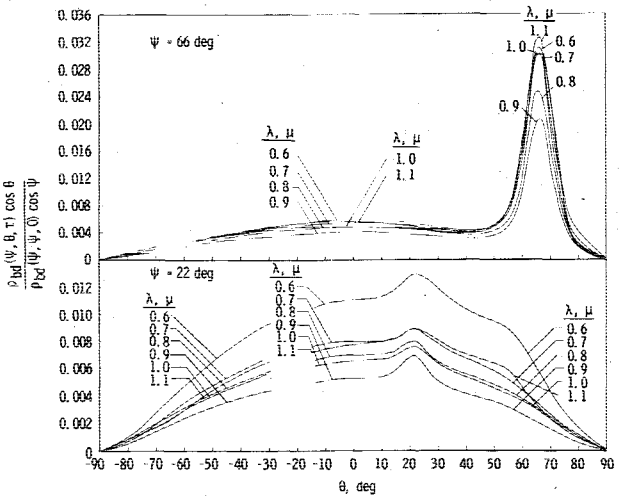

Fig. 6 Effect of irradiance wavelength on the bidirectional reflectance of a 1000-μ-thick H_2O film on a polished copper substrate for incidence angles of 22 and 66 deg.

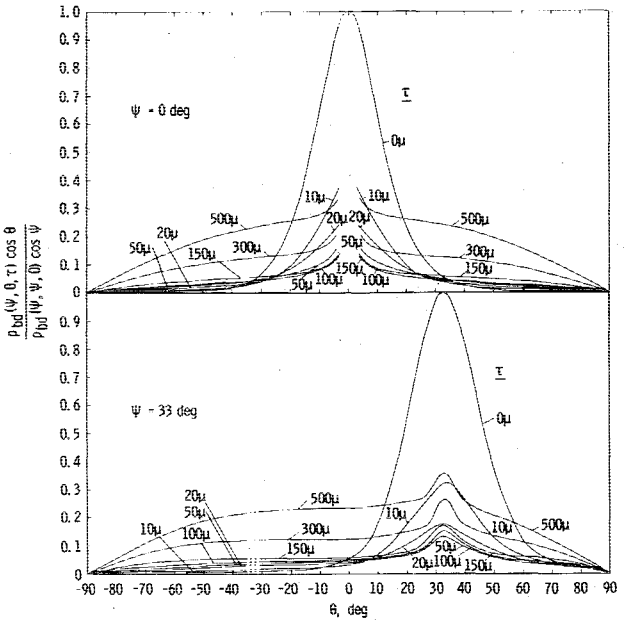

Fig. 7 Bidirectional reflectance of visible and near-infrared radiation from various thicknesses of H_2O cryofilms on a black epoxy paint substrate for incidence angles of 0 and 33 deg.

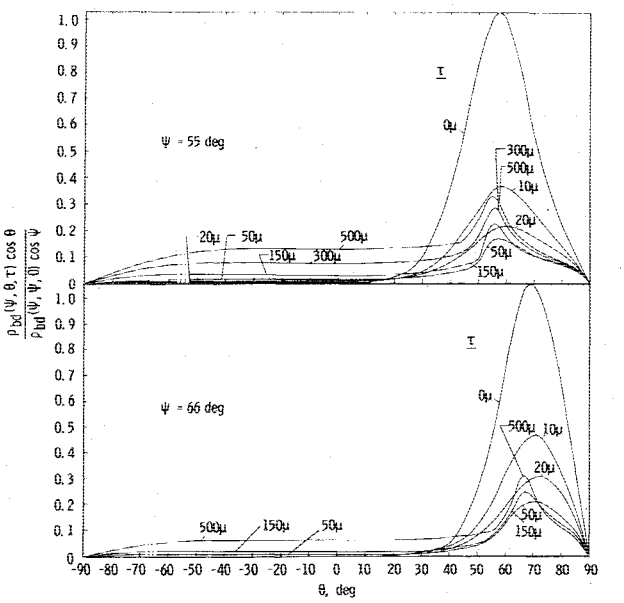

Fig. 8 Bidirectional reflectance of visible and near-infrared radiation from various thicknesses of H_2O cryofilms on a black epoxy paint substrate for incidence angles of 55 and 66 deg.

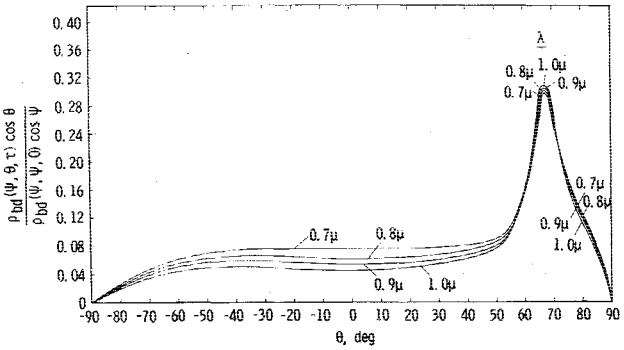

Fig. 9 Effect of irradiance wavelength on the bidirectional reflectance of a 500-μ-thick H_2O film on a black epoxy paint substrate for an incidence angle of 66 deg.

Figure 9 presents the effect of irradiance wavelength on the bidirectional reflectance of a 500-μ-thick H_2O film on black paint. The results shown are for an incidence angle of 66 deg. Note that the bidirectional reflectance for the H_2O film decreases as irradiance wavelength increases for reflection angles away from the vicinity of the specular peak. This reduction in the bidirectional reflectance is attributed to a decrease in internal scattering with increasing wavelength. It also is shown in Fig. 9 that the specular peak, which is due to specular reflection off the vacuum-film interface, increases in magnitude as the irradiance wavelength becomes larger. Such behavior is consistent with the wavelength dependence predicted and measured[8,9] for specular reflection from roughened dielectric interfaces, $\exp[-(4\pi\sigma\cos\psi/\lambda)^2]$. The specular reflection dependence on wavelength and incidence angle given by this function also explains why the specular peak observed for $\lambda=1.1$ μ in Fig. 6 is greater than that observed for $\lambda=0.6$ μ when $\psi=66$ deg but not when $\psi=22$ deg.

In Fig. 9, no indication of an absorption band is evident for the specular or nonspecular directions. The films in Figs. 9 and 6 were formed under similar experimental conditions, i.e., a deposition pressure of 4×10^{-4} Torr and a deposition rate of 0.044 μ/s. An immediate question that comes to mind is, why should one film exhibit an absorption band at 0.9 μ whereas the other does not? The explanation for such behavior probably can be attributed to the crystal size and/or shape. A similar spectral trend in the reflectance of snow cover for this wavelength region was shown by Dunkle and Bevans[10] in which the prominence of the absorption band was found to increase with increasing particle size.

Superspecular Maxima in Bidirectional Reflectance

As shown in Fig. 8, superspecular maxima are observed in the visible and near-IR bidirectional reflectance results for H_2O films on black epoxy paint. These maxima occur at reflection angles θ_p that are greater than the specular reflection angle, $\theta=\psi$, and appear only for large incidence angles, as indicated by comparison of Fig. 7 with Fig. 8. In Fig. 7, which is for $\psi=0$ deg and 33 deg, no superspecular maxima are observed in the reflection distributions. However, in Fig. 8, which is for $\psi=55$ and 66 deg, superspecular maxima are present in the reflection distributions for the bare substrate and also are observed in the reflection distributions for H_2O film thicknesses up to and including 50 μ. It also is noted in Fig. 8 that the difference between the angular locations of the superspecular maxima and the specular direction, $\Delta\theta=\theta_p-\psi$, depends upon the thickness of the film. This is illustrated better in Fig. 10, where $\Delta\theta$ for an incidence angle of 66 deg is displayed as a function of film thickness for H_2O films on black paint. The results shown for the H_2O films are for 0.9-μ wavelength and are taken from the reflection distributions for films formed at deposition rates of 0.012, 0.044, and 0.098 μ/s. From these data, it appears that there is not an appreciable effect of deposition rate on the angular displacements of the superspecular maxima. It is shown in Fig. 10 that the angular displacement of the superspecular maxima relative to the specular direction increases from 3 deg up to a maximum of 7 deg as the film thickness increases from 0 to approximately 25 μ. When the film thickness increases above 25 μ, the angular displacement of the superspecular maxima begins to decrease. An example of this decrease may be seen in Fig. 8 by comparing the reflection distributions for 20- and 50-μ films. It is further observed in Fig. 10 that an additional increase in the film thickness causes a continuing decrease in the angular displacement of superspecular maxima. As the film thickness approaches 150 μ, the superspecular maxima merges with the arising specular peak. This can be seen, for example, in the 150-μ H_2O reflection distribution of Fig. 8. Further increase of the film thickness above 150 μ causes the magnitude of the specular peak to rise in a manner similar to that observed for the 150- to 500-μ thickness increase in Fig. 8. The resulting 500-μ reflectance distribution for $\lambda=0.9$ and $\dot{\tau}=0.044$ μ/s is shown in Fig. 9.

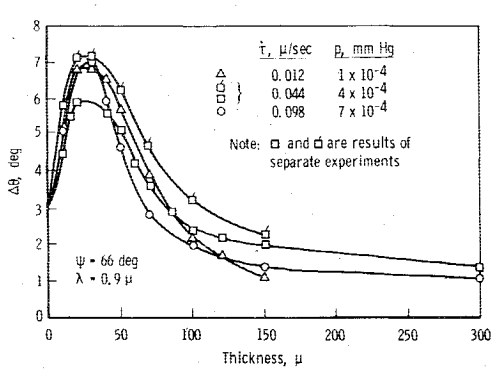

Fig. 10 Angular displacement of the superspecular maxima relative to the specular direction for various thicknesses of H_2O films on a black epoxy paint substrate for $\lambda=0.9$ μ and $\psi=66$ deg.

The appearance, for large incidence angles, of superspecular maxima in reflection distributions has been observed previously[11] for rough dielectric surfaces with a σ/λ ratio somewhat larger than unity. An explanation of this phenomenon is presented in Ref. 11 and is based on a representation of the rough dielectric surface as an aggregate of microscopic facets with different inclinations, each of which reflects radiation in accordance with the laws of geometrical optics. It is shown in Ref. 11 that the occurrence of superspecular maxima in the reflection distributions can be attributed fully to local Fresnel reflection from microscopic facets that have relatively small inclinations with respect to the macroscopic surface. From this information, the occurrence of superspecular maxima for H_2O cryofilms formed on a black epoxy paint substrate, as shown in Fig. 8, and the dependence of their angular location on film thickness, as shown in Fig. 10, can possibly be explained as follows. It is speculated that the rms roughness of the surface of the black paint substrate was comparable to or greater than the wavelength of the incident radiation, and the rms inclination of the microscopic facets comprising this surface, although small, was large enough to cause the superspecular maxima observed in Fig. 8 for the bare substrate. It is postulated further that the top surface of the thin cryofilms formed on the black paint substrate was even rougher than the substrate surface, and thus the rms facet inclination for the cryofilm surface was larger than the rms facet inclination for the bare paint surface. If this postulate is correct, the angular displacement of the superspecular maxima relative to the specular direction should be larger, as is observed for the 10-μ films in Figs. 8 and 10. The increase in the angular displacement of the superspecular maxima as the film thickened then indicated that the film surface became increasingly rough, and its rms facet inclination increased until apparently reaching some maximum value at a certain film thickness. The rms facet inclination, after attaining its maximum value, apparently decreased to a very low value with further increase in film thickness, since the angular displacement of the superspecular maxima decreased and became quite small, as shown in Fig. 10. This indicates that the H_2O film surface, after reaching a maximum roughness, became increasingly smoother with additional film thickness increase. Such behavior for the H_2O cryofilm surface is confirmed further by the emergence of a specular peak in the reflection distributions of Fig. 8 and the increase in the magnitude of this peak as the film thickened.

From the preceding discussion and the results in Fig. 10 for H_2O films, it appears that the surface profile characteristics of the substrate have a large effect on the surface profile characteristics of thin cryofilms but less influence on the surface profile characteristics of thick cryofilms. This ob-

servation is borne out further by noting that, in the reflection distribution results for the films formed on the polished copper substrate, no superspecular maxima ever occurred. In this case, the rms surface roughness of the substrate (0.01 μ) was much less than the wavelength of the incident radiation. Hence, the top surface of a thin film formed on the polished copper, although likely to be rougher than the substrate surface, probably would not have an rms facet inclination large enough to cause a superspecular maxima. However, as the film thickened, its surface would become rougher, and the rms facet inclination would increase to a value that might be large enough to produce a superspecular maxima. For the films formed on polished copper, it is speculated that the film surface became rougher and the rms facet inclination increased with thickness until reaching a limiting value, which was not large enough to cause a superspecular maxima. Hence, the surface of the H_2O film, although rougher than that of the copper substrate, was relatively smooth compared to the wavelength of the incident radiation. This is confirmed somewhat by the fact that water cryofilms formed at 77 K and low pressures have the form of vitreous ice, and x-ray diffraction studies of these films in Ref. 12 indicate that they have an amorphous structure and thus a relatively smooth surface.

Summary

From the bidirectional reflectance measurements, it is found that the presence of H_2O cryofilms on a polished copper or black paint surface causes radiation to be reflected more diffusely. For an H_2O film, the reflection distribution retains a significant specular peak even at a film thickness of 500 μ. Also, superspecular maxima are observed in the reflection distributions for H_2O cryofilms on black paint substrates, and the angular location of these maxima relative to the specular direction is found to be a function of film thickness and irradiation incidence angle. In addition, the experimental results indicate that thin H_2O cryofilms backscatter significantly for large incidence angles. Also, scattering interference patterns are seen in the bidirectional reflection measurements for H_2O cryofilms formed on polished copper.

Acknowledgment

The research reported herein was performed by the Arnold Engineering Development Center (AEDC), Air Force Systems Command (AFSC). Work and analysis for this research was done by personnel of ARO, Inc., a Sverdrup Corporation Company, operating contractor of AEDC.

References

[1] Wood, B. E., Smith, A. M., Roux, J. A., and Seiber, B. A., "Spectral Infrared Reflectance of H_2O Condensed on LN_2-Cooled Surfaces in Vacuum," *AIAA Journal*, Vol. 9, Sept. 1971, pp. 1836-1842.

[2] Wood, B. E., Smith, A. M., Roux, J. A., and Seiber, B. A., "Spectral Absolute Reflectance of CO_2 Frosts from 0.5 to 12.0 μ," *AIAA Journal*, Vol. 9, July 1971, pp. 1338-1344.

[3] Smith, A. M., Tempelmeyer, K. E., Müller, P. R., and Wood, B. E., "Angular Distribution of Visible and Near IR Radiation Reflected from CO_2 Cryodeposits," *AIAA Journal*, Vol. 7, Dec. 1969, pp. 2274-2280.

[4] Smith, A. M. and Wood, B. E., "Bidirectional Reflectance of Specular and Diffusing Surfaces Contaminated with CO_2 Cryofilms," *Progress in Astronautics and Aeronautics: Thermophysics of Spacecraft and Outer Planet Entry Probes*, Vol. 56, edited by A. M. Smith, AIAA, New York, 1977, pp. 157-173.

[5] Tempelmeyer, K. E. and Mills, D. W., Jr., "Refractive Index of Carbon Dioxide Cryodeposit," *Journal of Applied Physics*, Vol. 39, May 1968, pp. 2968-2969.

[6] Wood, B. E. and Smith, A. M., "Spectral Reflectance of Water and Carbon Dioxide Cryodeposits from 0.36 to 1.15 μ," *AIAA Journal*, Vol. 6, July 1968, pp. 1362-1367.

[7] Smith, A. M., Müller, P. R., Frost, W., and Hsia, H. M., "Super- and Subspecular Maxima in the Angular Distribution of Polarized Radiation Reflected from Roughened Dielectric Surfaces," *Progress in Astronautics and Aeronautics: Heat Transfer and Spacecraft Thermal Control*, Vol. 24, edited by J. W. Lucas, AIAA, New York, 1970, pp. 249-269.

[8] Chinmayanandam, T. K., "On the Specular Reflection from Rough Surfaces," *Physical Review*, Vol. 13, Feb. 1919, pp. 96-101.

[9] Toporets, A. S., "Specular Reflection from a Rough Surface," *Optics and Spectroscopy*, Vol. 16, Jan. 1964, pp. 54-58.

[10] Dunkle, R. V. and Bevans, J. T., "An Approximate Analysis of the Solar Reflectance and Transmittance of a Snow Cover," *Journal of Meteorology*, Vol. 13, April 1956, pp. 212-216.

[11] Voishvillo, N. O., "Reflection of Light by a Rough Glass Surface at Large Angles of Incidence of the Illuminating Beam," *Optics and Spectroscopy*, Vol. 22, June 1967, pp. 517-520.

[12] Dowell, L. G. and Rinfret, A. P., "Low-Temperature Forms of Ice as Studied by X-ray Diffraction," *Nature*, Vol. 188, Dec. 31, 1960, pp. 1144-1148.